

ESTIMATION OF THE LOADING CONDITIONS TO FRACTURE BEHAVIOUR

¹Gintautas DUNDULIS, ¹Evaldas NARVYDAS, ¹Vitalis LEIŠIS, ²Tom PETIT

¹*Kaunas University of Technology, Kaunas, Lithuania, EU, Gintautas.Dundulis@ktu.lt*

²*Université Paris-Saclay, CEA, Service d'Etude des Matériaux Irradiés, Gif-sur-Yvette, France, EU*

<https://doi.org/10.37904/metal.2022.4409>

Abstract

FRACTESUS (Fracture mechanics testing of irradiated RPV steels by means of sub-sized specimens) is a project supported by the European Commission HORIZON2020 programme. The project started in October of 2020 and will be finished in September of 2024. Twenty-two organizations from across Europe (15), Switzerland (1), United Kingdom (3), Japan (1), United State (1) and Canada (1) are participating in this project. The goal of this project is to join European and International effort to establish the foundation of small specimen fracture toughness validation and demonstration to achieve change in code and standards allowing address the various national regulatory authority concerns.

One of the important tasks of this project is the experimental and numerical simulation of the fracture mechanical behavior of the sub-sized specimens. The numerical simulation of the J -integral, of the loss of constraint assessment and finally the evaluation of the size effect is being performed. These numerical simulations will help to rationalize the experimental data.

This paper presents the influence of simulated loading conditions and finite element mesh on J -integral. Two options were investigated of the load transfer to the specimen: by a pin with a zero friction and by added material chunk with the triangular tip. The evaluation of the size effect to the fracture behavior was presented also. For this purpose, the Finite Element (FE) code ANSYS was used.

The paper is for the dissemination of the project results.

Keywords: finite element method, fracture mechanic, J -integral, modelling of pin, size of specimen

1. INTRODUCTION

Fracture toughness is usually used as a generic term for measures of material resistance to extension of a crack. It is restricted to results of fracture mechanics tests in this work, which are directly applicable to fracture control and to fracture test in describing the material property for a crack to resist fracture. The application of fracture mechanics methods allow to assess the structural integrity assessment, damage tolerance design, fitness-for-service evaluation, and residual strength of the different engineering components and structures. The fracture toughness values may also serve as a basis in material characterization, performance evaluation, and quality assurance for dangerous to environment engineering structures including nuclear power plant components. Therefore, fracture toughness testing and evaluation has been a very important subject in development of fracture mechanics method and its engineering applications [1,2].

There are brittle and ductile types of fracture and each type is analyzed by linear elastic fracture mechanics (LEFM) or elastic-plastic fracture mechanics (EPFM) theories [1]. The stress intensity factor (SIF) is the parameter used in LEFM. Crack tip opening displacement (CTOD) and J -integral are the parameters used to describe the conditions of crack tip in EPFM and each can be used as fracture criterion.

In this paper it was calculated the increase in the value of the J integral as a function of the monotonic mechanical loading applied to the simulations, via the formulas given in the ASTM E1921 standard. The

automatically generated in a minor amount in case of mesh 2. These elements have a quadratic mathematical formulation for displacement interpolation, but the shape of tetrahedron with 10 nodes. For the choice of rigid pin, the CONTA174 and TARGE170 elements were used to simulate contact between the pin and specimen. Side view of the created meshes is presented in **Figure 2**.

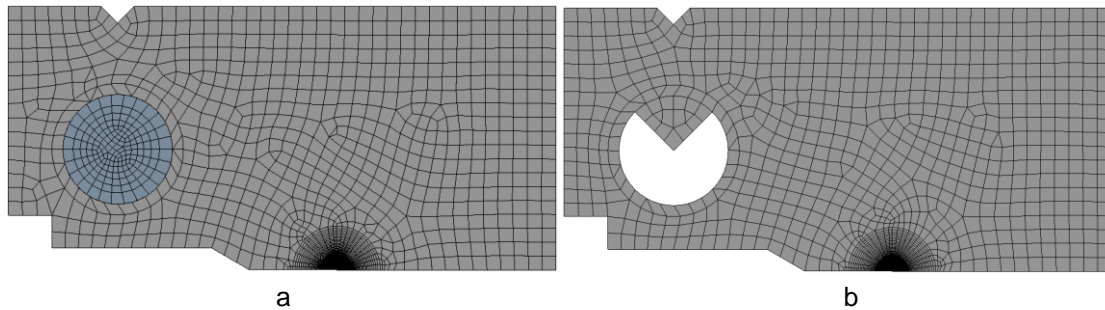


Figure 2 Mesh of choice 1 (a) and choice 2 (b) – side view

Major difference between mesh 1 and mesh 2 was in different approach to a number of finite elements across the thickness of the model. In mesh 1, the number of elements was 23 per thickness for sub-sized model (**Figure 3 a**) and 40 elements for CT model (**Table 1**). These numbers of elements were the same for the entire shape of the models. The mesh was refined toward the external side of the model. In mesh 2, the number of elements was 8 per thickness for sub-sized model (**Figure 3 b**) and the same number for CT model. However, the number of elements per thickness at the vicinity of the crack tip was increased to 19 for the sub-sized specimen model and to 25 for the CT model. The mesh was also refined toward the external side of the model.

Modelling of the pre-crack was performed by using a notch with a radius of curvature R_0 ($R_0 = 0.005$ in **Figure 1**, also see **Figure 4**). This method ensures the convergence of the mesh if R_0 is chosen small enough [6,7,8].

It is very important to mesh the crack tip correctly for modelling of fracture parameters. It is recommended [6] to perform the analysis using brick shape elements created in circular pattern around crack tip. The prism shape elements can also be used, especially when modeling sharp crack tip. The side view of the meshed model is shown in **Figure 4**. Refined zone at the crack tip was identical for CT and sub-sized models.

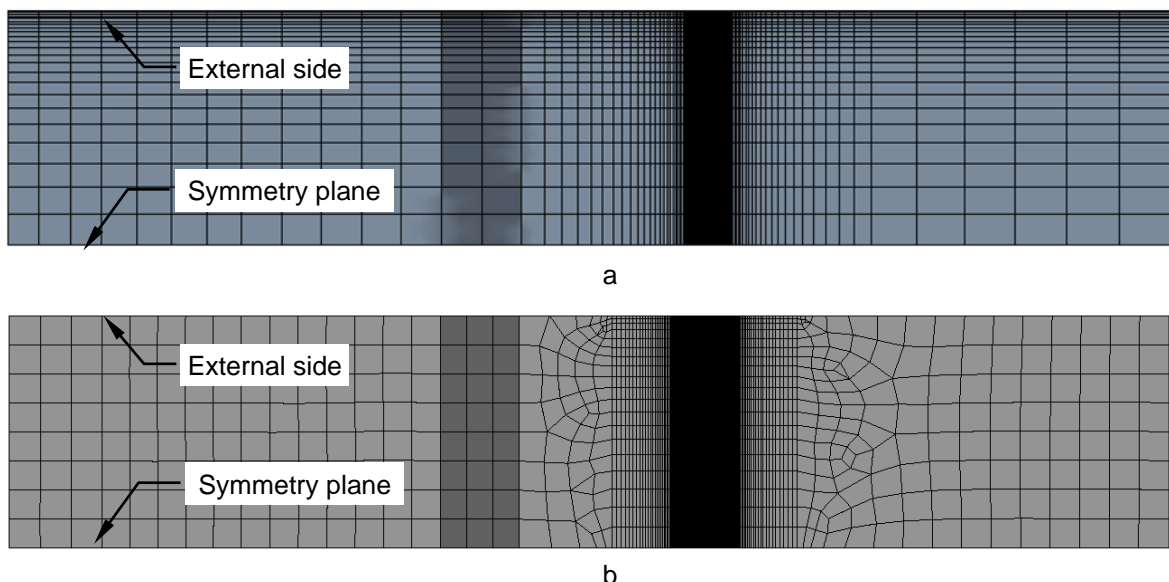


Figure 3 Finite element mesh 1 (a) and mesh 2 (b) on the crack plane

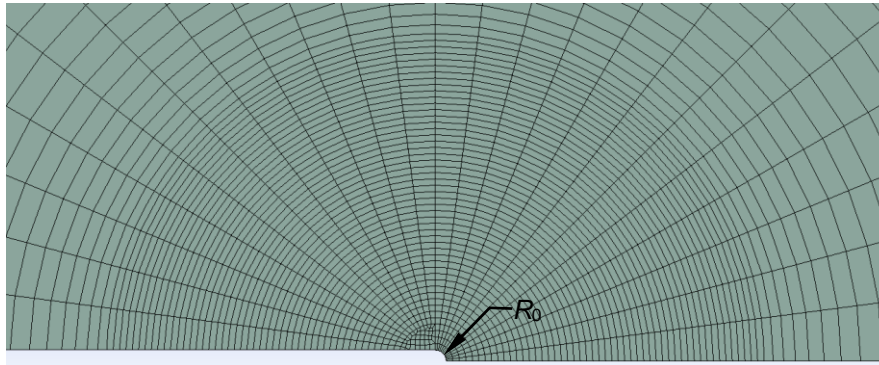


Figure 4 Side view of the mesh at the crack tip

Table 1 Mesh statistics of finite element models and elapsed time of solution

Model type		Mesh 1				Mesh 2			
		Elements	Nodes	No of elements per thickness	Elapsed time(hrs)	Elements	Nodes	No of elements per thickness	Elapsed time (hrs.)
CT	Choice 1	100790	429291	40	52.8	53973	224658	25 (8)	7.30
	Choice 2	101160	431462	40	42.8	53691	222690	25 (8)	4.76
MCT	Choice 1	54349	235466	23	6.6	42358	178960	19 (8)	3.75
	Choice 2	53475	231644	23	6.2	40889	172379	19 (8)	3.40

2.2. Material properties

Material state is considered corresponding to RPV steel mechanical properties at 23 °C. The parameters for isotropic elasticity (Young's modulus and Poisson's ratio) and isotropic multilinear hardening (multilinear curve data for plastic strain range from 0 to 0.7 with 0.02 spacing) are delivered. For the pin material (choice 1) following parameters were applied: Poisson's ratio $\nu_{pin} = 0.3$ and large $E_{pin} = 999999999$ MPa Young's modulus. The same material properties were used for the additional material chunk with a triangular tip (choice 2). Isotropic elasticity parameters of the main material are given in **Table 2**

Table 2 Mechanical properties of the main material (RPV steel at 23 °C)

E (MPa)	ν	Yield stress (MPa)
202563	0.3	487

3. CALCULATION RESULTS

Primary results of finite element simulation were force reaction (P) at the load location versus crack mouth opening displacement (CMOD). These results were used to calculate J -integral according to ASTM E1921 standard by equations:

$$J = J_e + J_p \quad (1)$$

$$J_e = \frac{(1-\nu^2)K_e^2}{E} \quad (2)$$

$$J_p = \frac{\eta A_p}{B_N b_0}, \quad A_p = A - 1/2 C_0 P^2, \quad \eta = 2 + 0.522 b_0 / W \quad (3)$$

where: A is the area under $P - \text{CMOD}$ curve; C_0 - the reciprocal of the initial elastic slope of the $P - \text{CMOD}$ curve, b_0 - initial remaining ligament, B_N - thickness dimension.

The comparison of J -integral and P results under maximum load for specimen CT and MCT are presented in **Table 3**. **Figure 5** presents P as load (a) and J -integral (b) versus crack mouth opening displacement curves of 3D FE models.

Table 3 J -integral and P values under maximum load for material at 23 °C

Specimen	Pin model	ANSYS mesh 1		ANSYS mesh 2		Difference between mesh 1 and mesh 2 (%)
		J -integral, (kN / m)	Difference between choice 1 and choice 2(%)	J -integral, (kN / m)	Difference between choice 1 and choice 2 (%)	
CT	Choice 1	302.7	3.3	302.6	2.9	0.03
	Choice 2	292.9		294.0		0.4
MCT	Choice 1	151.8	0.6	152.6	0.3	0.5
	Choice 2	150.9		152.1		0.8
		P , N		P , N		
CT	Choice 1	77610	0.3	77516	0.2	0.1
	Choice 2	77410		77348		0.1
MCT	Choice 1	2092	0.1	2094	0.05	0.1
	Choice 2	2090		2093		0.1

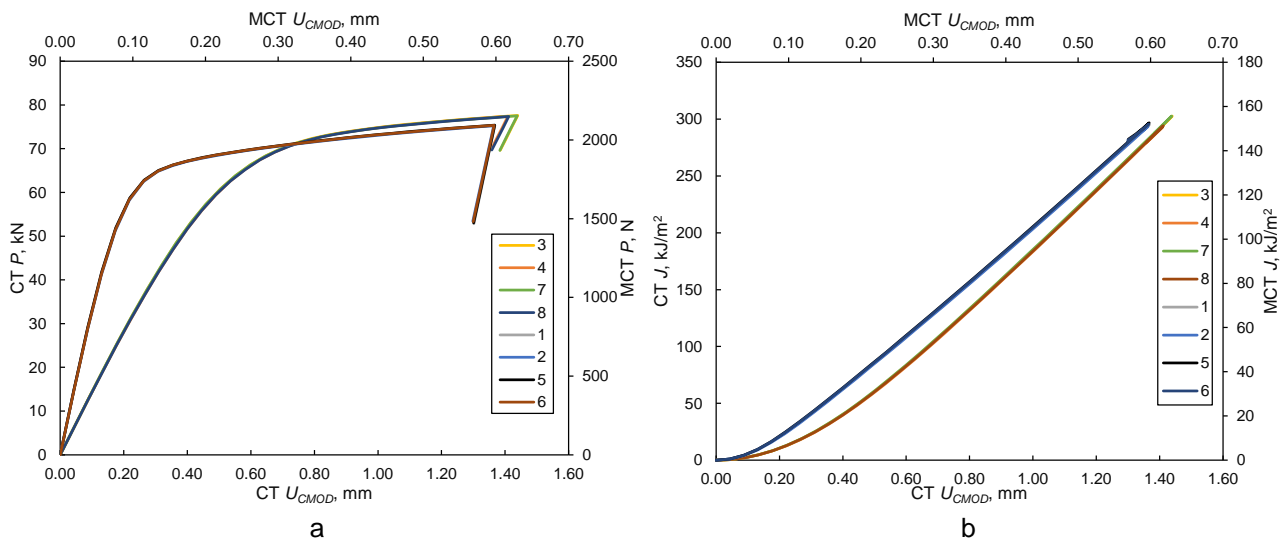


Figure 5 Numerically determined load (a) and J -integral (b) vs CMOD: specimen CT, Choice 1: 3 – Mesh 1, 7 – Mesh 2; Choice 2: 4 – Mesh 1, 8 – Mesh 2; specimen MCT, Choice 1: 1 – Mesh 1, 5 – Mesh 2; Choice 2: 2 – Mesh 1, 6 – Mesh 2

The influence of simulated loading conditions and finite element mesh on the stress field in the vicinity of the crack front and J -integral was analysed. As it was explained before four options were investigated: two load transfer choices and two different meshes. It was found that the different meshing has a negligible (less than 1% difference) influence to numerical P , $P - \text{CMOD}$, and subsequently J -integral results. The more influence

(3.3% and 2.9% differences) was found comparing J -integral values under maximum load between stiff pin and additional material chunk options (choice 1 and choice 2) for CT specimen.

4. CONCLUSION

The numerical investigations of the Compact Tension (CT) and sub-sized Miniature Compact Tension (MCT) specimens were performed for the estimation of J -integral for the RPV steel. The finite element method was used for the numerical investigation using the state-of-the-art ANSYS code. Primary result of finite element simulation was force reaction (P) and after, the P -CMOD curve was used to calculate J -integral according to ASTM E1921 standard.

Two options of load transfer and two finite element meshes were used in modelling of CT and MCT specimens for P and J -integral calculation. The largest ~3% difference was found comparing J -integral values under maximum load between stiff pin and additional material chunk options (choice 1 and choice 2). Other results demonstrated negligible less than 1 % difference between analysed cases. It was estimated that load transfer choice has small influence to analysis results and any choice can be used in modelling of load transfer.

The mesh choices with different approach to number of finite elements across the thickness of the model have negligible influence to the presented analysis results. Therefore, the models of choice 2 and mesh case 2 are suggested for the presented purpose. However, it is very important to mesh the crack tip correctly for modelling of fracture parameters. It is recommended to mesh it using brick shape elements created in circular pattern around crack tip.

ACKNOWLEDGEMENTS

The authors gratefully acknowledge the FRACTESUS consortium for providing the data and the expert panel for the assessment of the individual data sets. This project has received funding from the Euratom Research and Training Programme 2014-2018 under Grant Agreement No. 900014.

REFERENCES

- [1] ANDERSEN, T.L. *Fracture Mechanics. Fundamentals and Applications*. Boca Raton, Ann Arbor, Boston: CRC Press Inc, 1991, 793 p.
- [2] ZHU, Xian-Kui and JOYCE, James A. Review of fracture toughness (G, K, J, CTOD, CTOA) testing and standardization. *Engineering Fracture Mechanics*. 2012, vol. 85, pp 1-46.
- [3] ASTM E1921-19a, *Standard Test Method for Determination of Reference Temperature, T_0 , for Ferritic Steels in the Transition Range*. ASTM International, West Conshohocken, PA, USA, 2019.
- [4] ASTM E1820-15a. *Standard Test Method for Measurement of Fracture Toughness*. ASTM International, West Conshohocken, PA, USA, 2014.
- [5] ANSYS Element reference, Version 2020 R2.
- [6] RUGGIERI, Claudio, DODDS, Robert H. Jr. A local approach to cleavage fracture modeling: An overview of progress and challenges for engineering applications. *Engineering Fracture Mechanics*. 2018, vol. 187, pp 381-403.
- [7] GAO, X., RUGGIERI, C., DODDS, R.H.Jr. Calibration of Weibull stress parameters using fracture toughness data. *International Journal of Fracture*. 1998, vol. 92, pp 175-200.
- [8] MCMEEKING, R.M. Finite deformation analysis of crack-tip opening in elastic-plastic materials and implications for fracture. *Journal of the Mechanics and Physics of Solids*. 1997, vol. 25, no. 5, pp 357-381.